

Overflow for the Complete Failure of the Downstream Shell of a Rockfill Dam

R.M. Alves¹, M.Á. Toledo¹ and R. Morán^{1,2}

¹Civil Engineering Department: Hydraulics, Energy and Environment
Technical University of Madrid. ETS de Ingenieros de Caminos, Canales y Puertos
Profesor Aranguren s/n, 28040 Madrid
Spain

²CIMNE - Centre Internacional de Metodes Numerics en Enginyeria
Campus Norte UPC, Gran Capitán s/n, 08034 Barcelona
Spain

E-mail: rmonteiro@caminos.upm.es

ABSTRACT

This paper presents the results of experimental research using physical models regarding the failure of the downstream shoulder of rockfill dams caused by overtopping. The aim of this investigation is to analyze how different parameters such as the rockfill permeability, the main geometric dimensions of the dam, or the impervious element type affect the flow that initiates failure and also the ultimate flow needed to break the downstream shell of the dam. The primary objective of this study is to develop predictive models for both discharge flows. For this purpose, tests with stepwise flow increments were performed by varying the rockfill size, the height and width of the dam, the downstream slope and the type of impervious element. The regression analysis was based on results from 61 experimental tests: 50 tests were used to calibrate the formulas and 11 were used for validation. The analysis shows that, for a given dam height, the failure and the initiation discharges depend essentially on the rockfill permeability and, to a lesser extent, on the slope of the downstream shell. The type of impervious element, central core, upstream face or the absence of this element, seems to have no significant effect.

Keywords: overtopping, rockfill dam, failure flow, dam protection.

1 INTRODUCTION

Consequences of overtopping of earth or rockfill dams can be catastrophic. According to the International Congress on Large Dams (ICOLD 1995), the main cause of failure for earth dams is overtopping, covering 31% of the total number of failures. It is also noted as the secondary agent in 18% of cases. The hazard analysis and description of historical dam failures due to overtopping can be found in literature (Harris 2015). As examples, the South Fork Dam (USA) failed in 1889 with 2,209 human casualties. Also, the Banqiao Dam (China) failed in 1975 causing around 171,000 fatalities and destroying the homes of 11 million people. This last failure is one of the most catastrophic events so far. In Spain, the most important socio-natural disaster of the twentieth century was caused by the failure of the Tous Dam in 1982 resulting in 20 to 25 deaths due to the flood or the dam break; more than 100,000 people were evacuated and economical losses were estimated at more than 330 million euro (Serra-Llobet et al. 2013).

Avoiding overtopping is, then, one of the biggest concerns when designing dams. However, it is important to understand the failure process: when does the failure begins?, how does it progresses?, which is the overtopping discharge needed to initiate and to complete the failure? so that one can forecast the potential affected areas or the hazard magnitude if overtopping were to occur. The subject is highly relevant in practice since rockfill dams are abundant among the highest and most risky embankment dams.

In a rockfill dam, the flows released during failure are controlled by the break of the impervious elements (Toledo et al. 2015a). However, this only occurs when the downstream shoulder is partially or totally washed out by the overflow. During overtopping events, the shell, designed to be dry, is subjected to intergranular flow that results in the raise of the saturation line, inducing water pressures that may lead to fail due to mass sliding. Mass sliding along the entire width of the dam or formation of erosion channels by particle dragging may occur, depending upon the downstream slope (Toledo et al. 2015b). Other studies on failure due to overtopping of dams using non-cohesive materials were carried out by Coleman et al. (2002), Franca and Almeida (2004), and Wishart (2007).

Limited research has been performed on this subject for rockfill dams, while most of the attention has been directed towards the erosion process of embankment dams that would be made up of cohesive materials. This research focused on analyzing the influence of geometric characteristics of the dam or the rockfill permeability on the overtopping flows needed to initiate and complete the failure of the downstream shell of the dam, which support the central core or upstream face. Once the shell fails, the failure of the impervious element and the uncontrolled release of reservoir water is usually imminent.

2 TEST SETUP, PROCEDURE AND MATERIALS

2.1 Test setup

The majority of tests analyzed herein were conducted in a straight channel 2.5 m wide, 1.4 m high and 13.7 m long located in the hydraulics laboratory of the *E.T.S de Ingenieros de Caminos, Canales y Puertos* of the Technical University of Madrid (UPM) (Figure 1). The channel is divided in four zones: Inlet and dissipation, testing, decantation (sediment collection), and return to the main tank (closed circuit). Starting from the upstream top, the zone for water supply and energy dissipation is formed by a hollow brick wall. The testing zone is located immediately downstream of this wall. Placed within one of the side walls is an inspection window 2.3 m long and 1.1 m high. This zone ends with a small gravel retention pond 1.35 m long and 0.10 m deep. The last zone is the drainage area that returns the water to the sump (270 m³), located below the laboratory. Tests were performed with three different dam widths: the total width of the channel and two longitudinal subdivisions of 0.60 m and 1.32 m wide. In addition, some tests were performed in a conventional testing channel 1.0 m wide of the Center of Hydrographic Studies of the CEDEX.

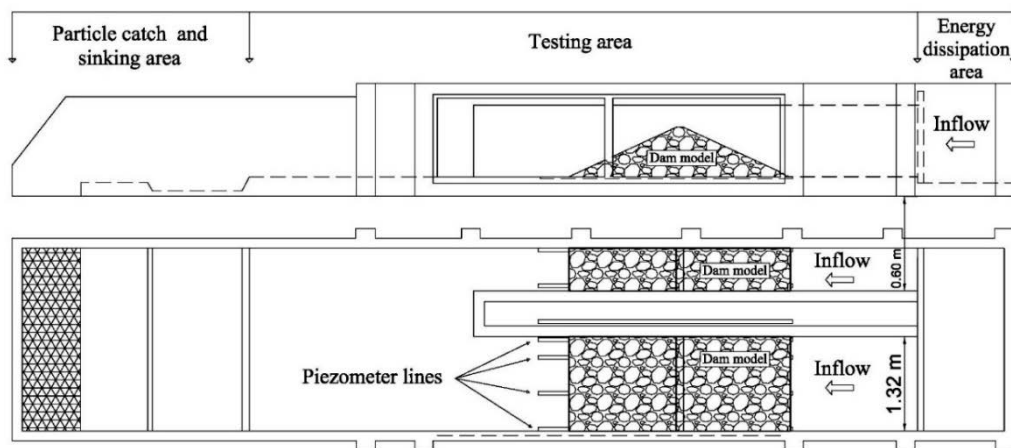


Figure 1. UPM channel used for the physical model tests.

2.2 Materials and impervious elements

Uniform crushed aggregates of different grain size were tested. For both gravels, the sieve size passing 50% of the particles (D_{50}) was 12.6 mm (M1) and 35.0 mm (M2). Figure 2 (left) shows the grain size distribution of each gravel and Table 1 summarizes basic characteristics. Both grain size distributions are quite uniform, with uniformity coefficients (C_u) of 1.55 and 1.58 for materials M1 and M2, respectively.

The size of the particles was selected so that a nonlinear relation between hydraulic gradient and seepage flow velocity was assured. The permeability characteristics of both materials were statistically calibrated using results of a test campaign specifically designed to obtain the nonlinear parameters. This experimental campaign consisted in nondestructive tests using downstream slopes constructed with the same materials (M1 and M2) subjected to water through flows increased step by step until total saturation of the rockfill shoulder was achieved. For each flow, the hydraulic head was measured in different points of the shoulder, what resulted in different combinations of hydraulic gradient and seepage velocity. The nonlinear resistance law of both materials is defined using Eq. **Error! Reference source not found.**

$$i=a\cdot v+b\cdot v^2 \quad (1)$$

where i represents the hydraulic gradient and v the seepage flow velocity. Parameters a and b were obtained for materials M1 and M2 and are summarized in Table 1.

During the test campaign, the failure process was analyzed for dams with no impervious element (SEI) and for dams with two different kinds of impervious elements: Upstream face (PI); modeled by a plastic screen placed over the upstream shoulder; Central core (CN); modeled by a masonry wall or by plastic screens placed over vertical metal grids.

Table 1. Basic characteristics of tested gravels.

Characteristics	M1	M2
D_{50} (mm)	12.6	35.0
Fine fraction (%)	-	0.1
Dry unit weight (kN/m ³)	14.3	14.3
Unit weight in saturated state (kN/m ³)	18.3	18.2
Void ratio (%)	69.0	71.0
Porosity (%)	41.0	41.8
Internal friction angle (°)	37	42
a (s/m)	2,71	0,82
b (s ² /m ²)	65,35	52,82

2.3 Test procedure and measurements

The rockfill dams were constructed without compaction. Tests were based on a stepwise flow increments methodology until total failure of the downstream shell occurred. The shell was considered completely failed when damage reached the dam crest. Each discharge was kept constant until steady state conditions were reached, *i.e.*, until no additional damage was observed on the shell or any change in the water elevations and pressures.

For each step, flows were measured upstream and downstream of the dam using, respectively, an ultrasonic flowmeter FLUXUS ADM7407 from FLEXIM GmbHTM located in the supply pipe and a rectangular weir located in the return channel to the sump. Flows measured with the flowmeter, used for this work, are mean values of the flows registered using a computer program during a period of time. This program have a recording frequency of approximately 0.25 Hz. The recording time of the discharges varied from test to test. The mean flow that used the minimum number of observations was calculated with 26 flows recorded over roughly 112 seconds. Not all tests were performed measuring both flow measurement devices. In those cases, flows were measured only using the rectangular weir. Although good agreement was observed between both measurement systems, in order to maintain a uniform criterion, flows obtained with the rectangular weir were corrected by means of an equation which reflects the relation between flows measured with the flowmeter and the rectangular weir (Figure 2, right).

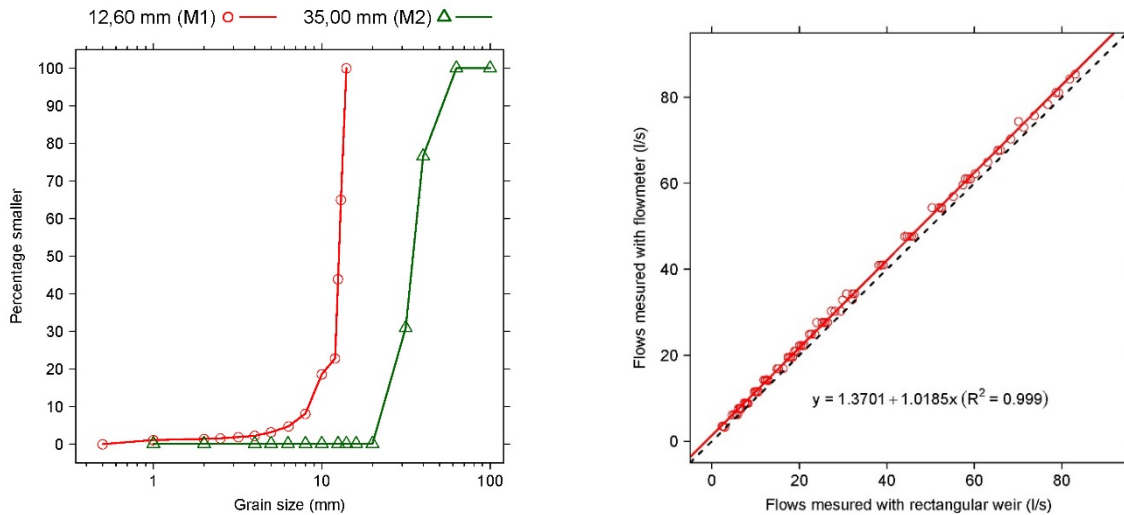


Figure 2. Particle size distributions for gravels M1 and M2 (left). Relation between flows measured with the flowmeter and the rectangular weir (right).

3 GOVERNING PARAMETERS

Figure 3 presents the parameters involved in the failure process of rockfill dams. These parameters are the height of the dam (H), the downstream slope ($N = H:V$), and the permeability characteristics of the dam. For a given discharge, failure begins at the toe of the dam and progresses upstream until it reaches the dam crest. An overtopping threshold should be overcome for the failure to initiate. The flow that initiates the failure is termed *Initiation discharge* (Q_i). Until this discharge is observed, no damage occurs to the dam. This period of time is termed *Incubation phase*. For practical purposes, in the analysis done in this work, the initiation flow is defined as the mean value between the first flow that produces damage to the dam and the last flow that does not produce any damage. The progress of the failure is characterized by the *Advance degree of failure* (ADF). For a given overtopping discharge, the ADF is the horizontal distance from the original toe of the dam to the most upstream point of the shoulder affected by failure (B). When this dimension equals the horizontal projection of the downstream slope (the failure reaches the dam crest), failure is considered complete. From this moment on, the impervious element is susceptible to be affected by the overflow. The discharge that produces the complete failure of the downstream slope is termed *Failure discharge* (Q_f). This flow is the mean value between the last flow rate that does not damage the crest of the dam and the first flow rate that damages the crest. The unit discharge (q) is the ratio between the total discharges (Q) and the width of the dam crest.

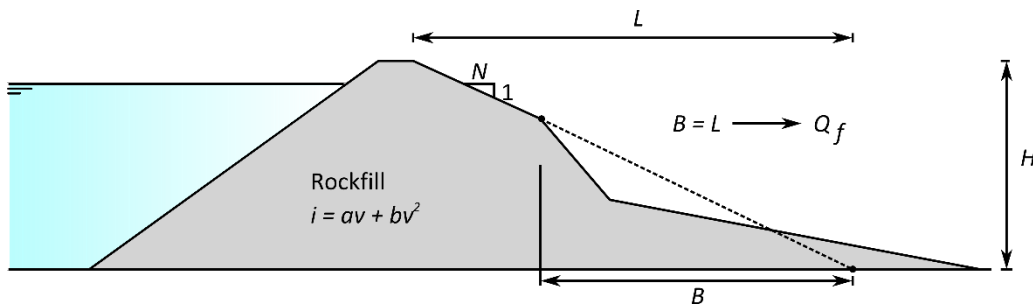


Figure 3. Parameters that govern the failure process.

Darcy's law is not applicable to flows through coarse granular materials where turbulence is observed. Nevertheless, in the toe of the dam, the equipotential lines calculated with the linear model are quasi-coincident with those obtained with nonlinear models. It is a consequence of the direction of the velocity vectors in this zone, approximately horizontal (for impervious foundations), what leads to equipotential lines almost vertical. In this zone, water pressure can be assumed as hydrostatic and the maximum gradients dependent only on the downstream slope. Comparing linear and non linear resistance formulas, there is only one point of coincidence between the flow gradient and the seepage velocity (Figure 4). So, the equivalent linear permeability coefficient must be selected taking into account the flow velocity field and the water pressures observed in the toe of the dam.

Assuming that the gradient in the toe of the dam is maximum and equal to $1/N$ (Toledo 1997), for a given rockfill placed in a downstream shoulder with slope N and subjected to through flow then, the equivalent linear permeability coefficient can be expressed by Eq. 2.

$$k_{eq} = \frac{v_{max}}{i_{max}} = \frac{\frac{-a + \sqrt{a^2 + 4b/N}}{2b}}{1/N} = \frac{N \cdot (-a + \sqrt{a^2 + 4b/N})}{2b} \quad (2)$$

In order to formulate regression models to estimate the unit initiation and failure discharges as functions of the geometric characteristics of the dam and the rockfill permeability, dimensional analysis was applied. The problem can be explained by four variables: the unit discharges (q), the height of the dam (H), the permeability of the rockfill (k_{eq}) and the acceleration of gravity (g). The height of the dam and the acceleration of gravity have independent dimensions so it is possible to select these parameters as basic variables. There are two basic dimensions explaining this problem, length (L) and time (T), so the four dimensional variables can be reduced to two non-dimensional variables. The dimensionless unit discharges (q^*) are expressed by Eq. **Error! Reference source not found.** and the dimensionless equivalent linear permeability coefficient (k_{eq}^*) by Eq. **Error! Reference source not found.**

$$q^* = \frac{q}{\sqrt{g \cdot H^3}} \quad (3)$$

$$k_{eq}^* = \frac{k_{eq}}{\sqrt{g \cdot H}} \quad (4)$$

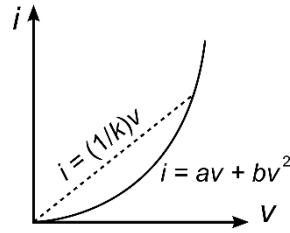


Figure 4. Comparison between the linear and nonlinear resistance formulas.

4 EXPERIMENTAL RESULTS

4.1 Failure and Initiation Discharges

When analyzing the effect of the different types of impervious elements on the unit failure discharge, it was observed that in most cases, for the same height of the dam and the same material type, tests using a central core (CN) needed a lower unit discharge to complete the failure of the downstream shoulder than tests using an upstream face (PI) or no impervious element (SEI) (Figure 5, left). The same figure shows that the unit failure discharges obtained for tests with an upstream face and tests with no impervious element were fairly similar. The same observation can be made for the unit initiation discharge (Figure 6, left).

The unit failure discharge clearly depends on the type of granular material used during the experimental campaign. In Figure 5 (right) it can be observed that both materials form two data clusters. Taking into account that both material are uniform, a larger rockfill size would have more permeable rockfill material requiring higher unit discharges for the complete failure of the downstream shell. These observations for the unit failure discharge also apply to the unit initiation discharge (Figure 6, right).

Variation of the unit failure discharge with the downstream slope have in general a positive trend (Figure 5 right) so, gentler slopes tend to be more resistant then steeper slopes. Different relationships can be obtained for each material used during the laboratory tests. For finer rockfills, this relation has a milder slope when fitting a linear regression. This means that the unit failure discharge of the physical models constructed with the coarser material have a greater dependency on the downstream slope. These observations for the unit failure discharge also apply to the unit initiation discharge. The positive trend of the unit failure discharge with the downstream slope is not

explicitly clear for experimental tests using dams that are 1 m high. Here, the downstream slope is of minor importance.

Influence of the height of the dam on the unit failure discharge is clear for tests using material M2. In this case, higher dams result in higher required discharges to break the downstream slope. Nevertheless, for tests using material M1, the importance of this variable vanishes. These observations can also be applied for the unit initiation discharge (Figure 6 right).

Summarizing, the unit failure discharge obtained for the physical models of material M1 seems to have a small dependency on the height of the dam and on the downstream slope. When using material M2, the unit failure discharge has a stronger and clearer dependency on both parameters. The unit initiation discharge for tests using material M1 depends mainly on the downstream slope while for tests with material M2 it depends also on the height of the dam, which is more as expected.

When using the dimensionless parameters obtained by dimensional analysis, it is possible to observe a direct correlation between the dimensionless unit failure discharge and the dimensionless equivalent linear permeability coefficient (Figure 7). Both the material type and the height of the dam follow the trend, as can be seen in the right and center images of Figure 7. So no additional effect of these variables over q_f^* should be taken into account in the formulation of a predictive model, *i.e.*, a clear relationship between q_f^* and k_{eq}^* exists. More permeable materials result in higher values of q_f^* . On the other hand, higher dams result in lower values of q_f^* . The effect of the downstream slope seems to have some relevance for the prediction of q_f^* since slopes within a certain range seem to form different data clouds that are roughly parallel (Figure 7, right). This observation suggests this parameter, the downstream slope, should be taken into account in a predictive model in order to improve its accuracy. The same observations can be made for the dimensionless unit initiation discharge (Figure 8).

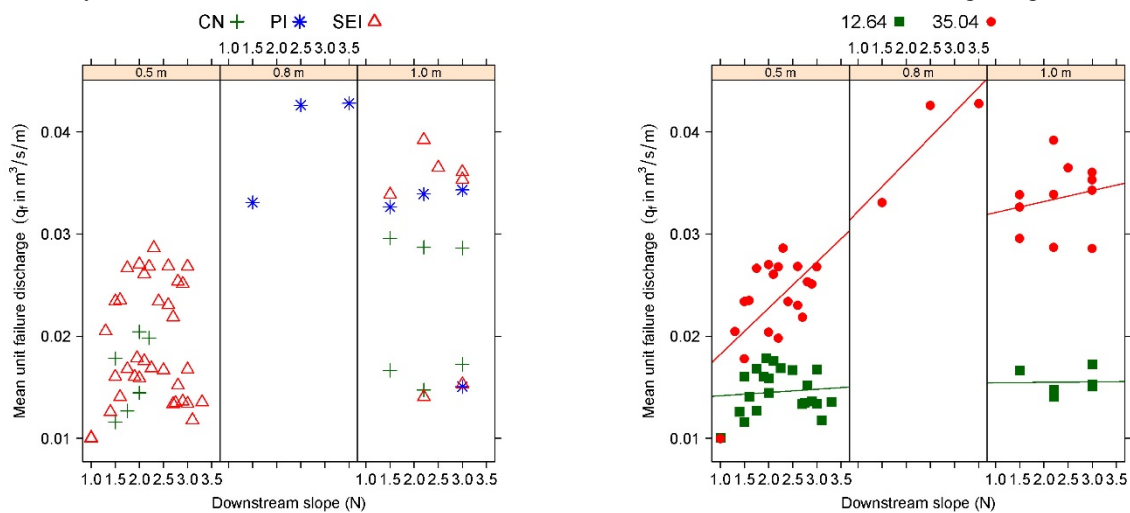


Figure 5. Variation of the unit failure discharge with the downstream slope distinguished by impervious elements and heights (left) and materials and heights (right). The subscript f stand for *failure*.

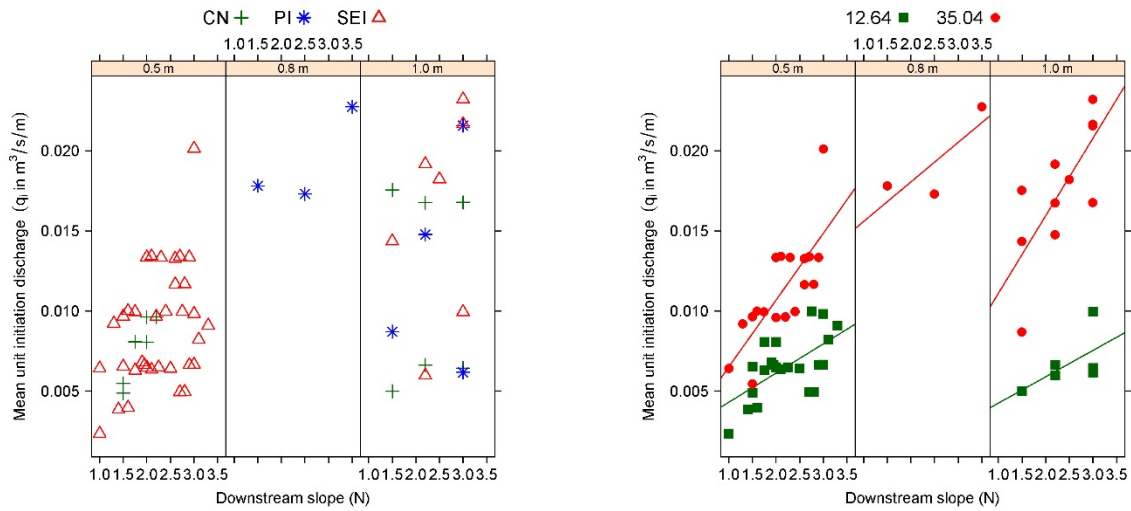


Figure 6. Variation of the unit failure discharge with the downstream slope distinguished by impervious elements and heights (left) and materials and heights (right). The subscript i stand for *initiation*.

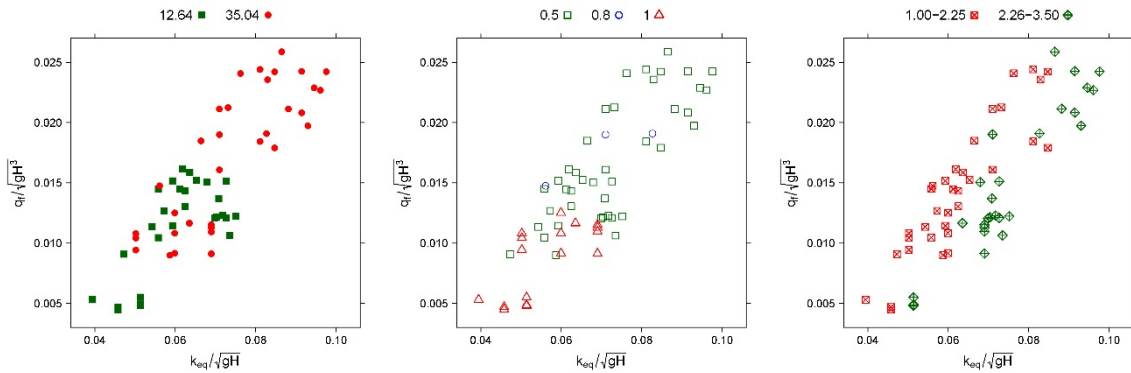


Figure 7. Variation of the dimensionless unit failure discharge with the dimensionless equivalent linear permeability coefficient distinguished by material types (left), dam height (center) and downstream slopes (right).

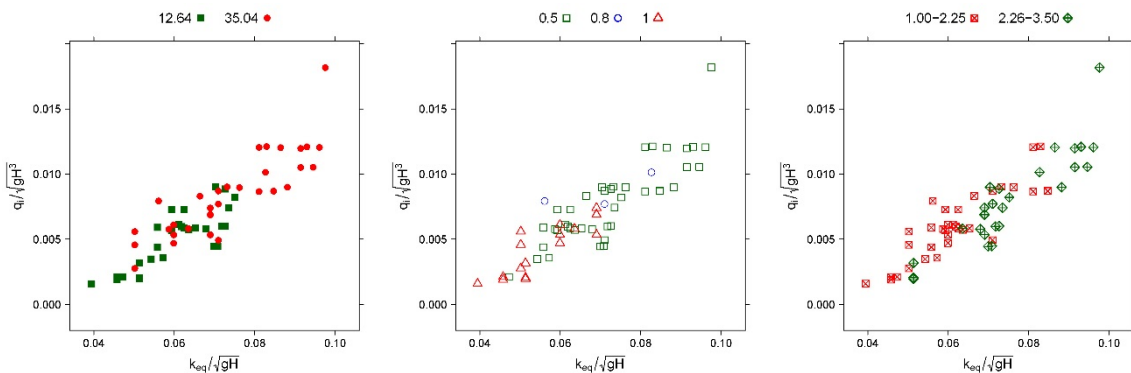


Figure 8. Variation of the dimensionless unit initiation discharge with the dimensionless equivalent linear permeability coefficient distinguished by material types (left), dam height (center) and downstream slopes (right).

4.2 Brittleness factor

The brittleness factor is defined as the ratio between the initiation unit discharge and the failure unit discharge. One of the most important observations is that, unlike for the initiation and failure discharges, the size of the gravel material does not affect the brittleness factor, as can be seen in Figure 9 (left). The brittleness factor also is not

dependent upon the type of impervious element (Figure 9, center). The scatterplots of each impervious element and each type of material used during the experiments are mixed together in a single data cloud where no dependence can be found. Relatively to the downstream slope, a positive dependency is found for the brittleness factor, as can be seen in Figure 9 (left and center). This relation is expressed by Eq. **Error! Reference source not found.**, with a low coefficient of determination ($R^2 = 0.245$).

$$BF = 0.2608 + 0.0951 \cdot N \quad (5)$$

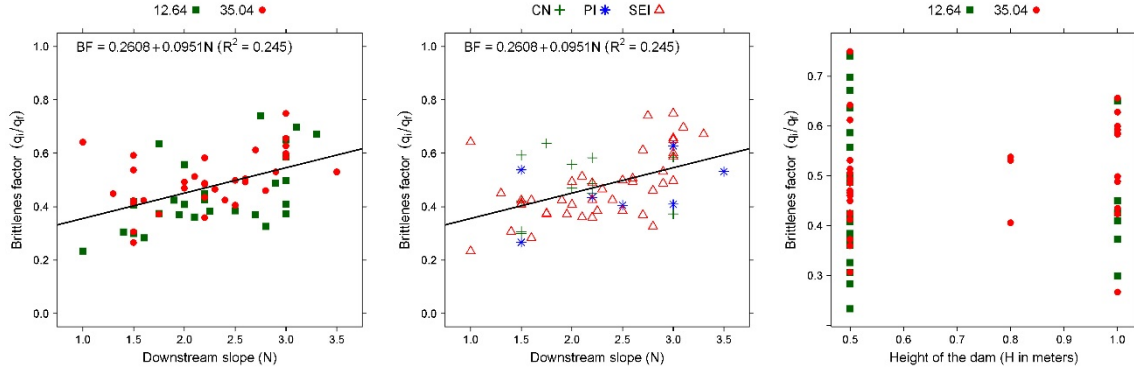


Figure 9. Relationship between the brittleness factor and the downstream slope distinguishing between material types (left), impervious elements (center) and heights. Relationship of the brittleness factor with the height of the dam (right). The subscripts *f* and *i* stand for *failure* and *initiation*.

5 PREDICTIVE MODELS

From the previous parametric analysis can be concluded that both the initiation and the failure discharges are mainly a function of the permeability characteristics of the rockfill (k_{eq}^*) as well as, to a lesser extent, a function of the dam downstream slope (N). Multiple linear regression models were fitted to estimate the dimensionless unit initiation and failure discharges (q^*) as a function of the variables k_{eq}^* and N (Eq. **Error! Reference source not found.**), where the coefficients c_1 , c_2 and c_3 were calibrated based on the test results.

$$q^* = c_1 + c_2 \cdot k_{eq}^* + c_3 \cdot N \quad (6)$$

To calibrate both predictive models 50 tests were used, and 11 tests were reserved for validation purpose (5 tests of material M1 and 6 of M2). The first tests of each material type from the original data frame were selected for validation.

The model proposed for the dimensionless unit failure discharge is expressed by Eq. **Error! Reference source not found.** for which the *mean relative error* (*MRE*) obtained is 2.6% with a standard deviation (*sd*) equal to 17.6% and $R^2 = 0.791$. For the dimensionless unit initiation discharge, expressed by Eq. **Error! Reference source not found.**, *MRE* is 5.4% with *sd* = 24.5% and $R^2 = 0.728$. These formulas can only be applied in the range of the tested values. The indicator *MRE* is the difference observed between the predicted discharges and those obtained experimentally with respect to these last discharges. Negative values refer to underestimation of the values.

$$q_f^* = -0.0049 + 0.4242 \cdot k_{eq}^* - 0.0041 \cdot N \quad (7)$$

$$q_i^* = -0.0062 + 0.2197 \cdot k_{eq}^* - 0.0008 \cdot N \quad (8)$$

The validation tests were compared to the predictive models (Figure 11). When comparing these tests with the dimensionless unit failure discharge model, the *MRE* was 1.8%, the standard deviation 11.3% and the modulus of the maximum relative error obtained was approximately 21.4%. For the initiation discharge model *MRE* = -4.2%, *sd* = 15.7% and the modulus of the maximum relative error was 29.6%.

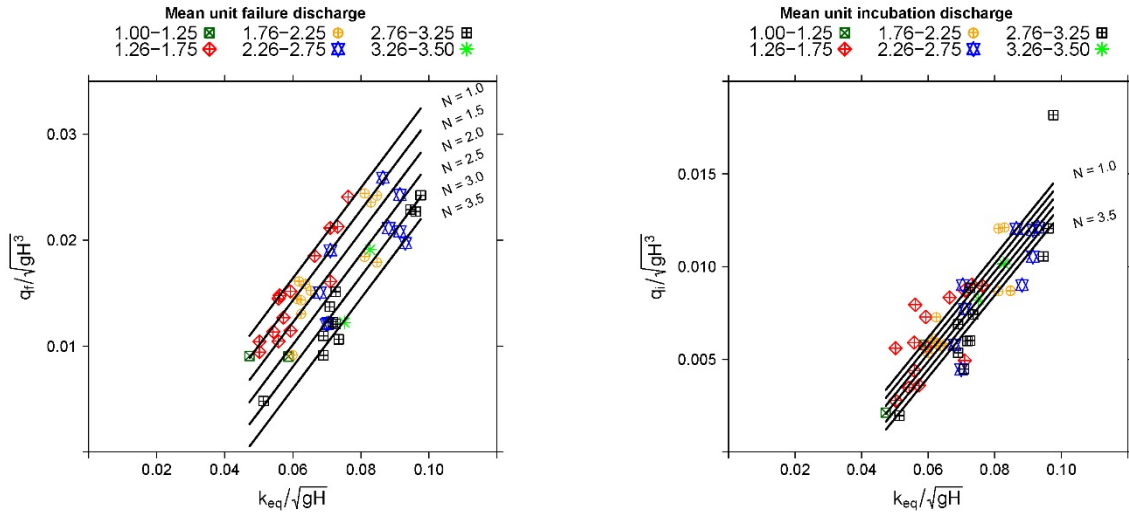


Figure 10. Variation of both dimensionless unit discharges with the dimensionless equivalent linear permeability coefficient for different downstream slopes (symbols above the graph).

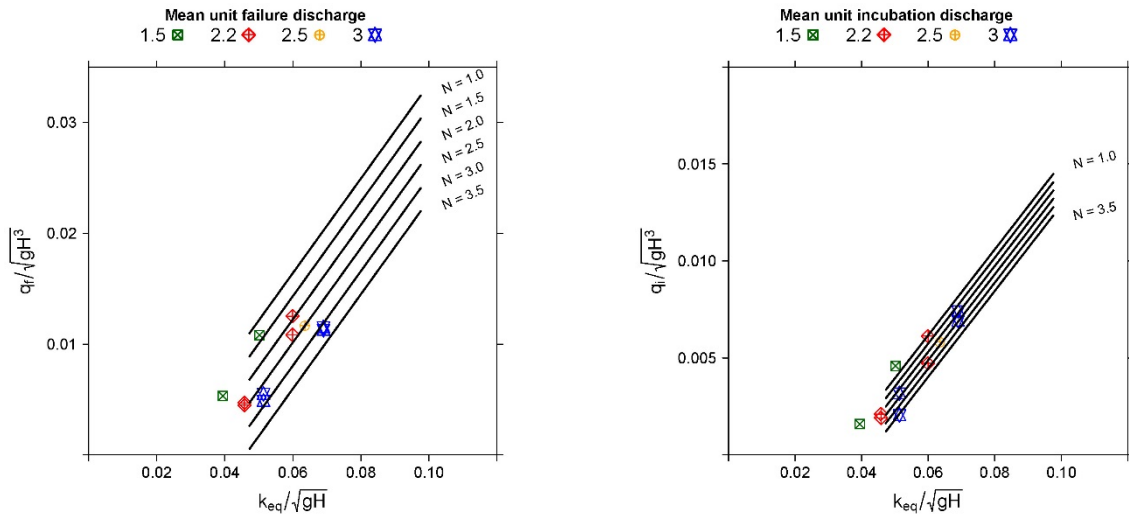


Figure 11. Comparison between the predicted discharges and those obtained experimentally.

6 DISCUSSION

From the parametric analysis it was possible to conclude that the two materials tested showed quite different initiation and failure discharges. According to the observation of the tests, it was assumed that the relevant parameter is the permeability of the rockfill. A rockfill with its size characterized by D_{50} may have different permeability depending on the size gradation. For a given D_{50} , a well graded material is expected to have a lower permeability than a uniform material, and consequently a higher elevation of the saturation line for the overtopping discharge analyzed. Therefore, failure of the downstream slope should be expected to occur for a lower discharge when comparing a rockfill dam of well graded material with another of uniform material.

The parametric analysis do not clearly explains the effect of the height of the dam on the unit initiation and failure discharges. A clear correlation is found between the unit initiation and failure discharges and the equivalent linear permeability coefficient. The downstream slope seems to play a minor role, though not negligible. So the prediction models should include k_{eq}^* and N as variables to predict q^* .

From a physical point of view, a material with permeability tending to zero (for example a very small uniform granular material) would need a very small amount of flow to saturate the downstream slope and to break it, so it should be expected that the failure flow tends to zero when the permeability tends to zero. The proposed formulas

are based in multiple linear regression models and that condition is not fulfilled. They can only be used in the range of data obtained from the tests, and additional work is necessary. The permeability coefficient of clean gravels may vary between 10^0 m/s and 10^{-2} m/s (Terzaghi et al. 1996). For a range of dam heights from 20 to 200 m, k_{eq}^* takes values between $2.3 \cdot 10^{-4}$ and $7.1 \cdot 10^{-2}$. A wide range of k_{eq}^* values are not covered by the proposed predictive models. An effort must be done in order to obtain a generic formulation that imperatively must converge to the origin of the graph.

The type of impervious element seems to have a minor effect over failure and initiation discharges. However, tests using a central core resulted in lower unit failure discharges than tests using an upstream face or no impervious element at all. A possible explanation for this observations could be the less amount of rockfill to saturate for the same overtopping discharge in the cases using a central core, what would imply a higher elevation of the saturation line. On the other hand, tests using upstream faces have longer flow lines that would result in lower hydraulic gradients that would also imply an elevation of the saturation line. Both physical effects oppose each other, and may give a negligible final effect.

With respect to the brittleness of rockfill dams failure, it was observed that it is mainly affected by the downstream slope and not by the type of material nor the height of the dam. For higher values of the downstream slope the rockfill dam becomes more fragile, *i.e.*, the difference between the initiation and the failure diminishes. This allows to conclude that independently from the rockfill characteristics, the impervious element or even the height of the dam, rockfill dams with gentler downstream slope behaves in a more brittle way.

7 CONCLUSIONS

The main conclusions of this experimental research work are:

- Both dimensionless unit initiation and failure discharges (q^*) are mostly affected by the dimensionless equivalent linear permeability coefficient (k_{eq}^*). The slope of the downstream shoulder of the dam (N) also affects the discharges but not in such an important way as k_{eq}^* . Higher values of N result in lower q^* while higher values of k_{eq}^* results in higher q^* .
- The type of the impervious element have a minor effect over the initiation or the failure discharges. However, a more detailed analysis should be carried out.
- The brittleness factor is mainly affected by the downstream slope of the rockfill dam. Dams with gentler slopes tend to be more fragile than those constructed with more steep slopes. Neither the permeability characteristics of the rockfill nor the height of the dam affect the brittleness factor.
- Predictive regression models based on the experimental results were obtained for estimating the failure and initiation discharges as a function of the permeability of the rockfill and the downstream slope for a given dam height. These models could only be applied when data are in the tested range.

8 ACKNOWLEDGMENTS

To Education and Science Ministry of Spain for financing the research project XPRES with the code BIA2007-68120-C03-01.

9 REFERENCES

- Coleman, S.E., Andrews, D.P., and Webby, M. G. (2002). "Overtopping Breaching of Noncohesive Homogeneous Embankments." *Journal of Hydraulic Engineering*, 128(9), 829–838.
- Franca, M.J., and Almeida, A.B. (2004). "A computational model of rockfill dam breaching caused by overtopping (RoDaB)." *Journal of Hydraulic Research*, 42(2), 197–206.
- Harris, M.J. (2015). "Failure of dams due to overtopping - A historical prospective." *Dam Protections against Overtopping and Accidental Leakage*, M. Á. Toledo, R. Morán, and E. Oñate, eds., CRC Press, Madrid, 73–81.
- ICOLD. (1995). *Bulletin 99 - Dam failures statistical analysis*. Paris, France.
- Serra-Llobet, A., Tàbara, J.D., and Sauri, D. (2013). "The Tous dam disaster of 1982 and the origins of integrated flood risk management in Spain." *Natural Hazards*, 65(3), 1981–1998.
- Terzaghi, K., Peck, R.B., and Mesri, G. (1996). *Soil Mechanics in Engineering Practice*. John Wiley & Sons.
- Toledo, M.Á. (1997). "Presas de escolleras sometidas a sobrevertido Estudio del movimiento del agua a través de

la escollera y de la estabilidad frente al deslizamiento en masa.” Universidad Politécnica de Madrid. E.T.S.I. Caminos, Canales y Puertos.

Toledo, M.Á., Alves, R.M., and Morán, R. (2015a). “Structural failure of the clay core or the upstream face of rockfill dams in overtopping scenario.” *Dam Protections against Overtopping and Accidental Leakage*, M. Á. Toledo, R. Morán, and E. Oñate, eds., CRC Press, Madrid.

Toledo, M.Á., Campos, H., Lara, Á., and Cobo, R. (2015b). “Failure of the downstream shoulder of rockfill dams in overtopping or accidental leakage scenario.” *Dam Protections against Overtopping and Accidental Leakage*², M. Á. Toledo, R. Morán, and E. Oñate, eds., CRC Press, Madrid, 89–99.

Wishart, J. (2007). “Overtopping breaching of rock-avalanche dams.” University of Canterbury.